Materials Research Express

PAPER • OPEN ACCESS

Menger fractal structure with negative refraction and sound tunnelling properties

To cite this article: Yu Liu *et al* 2019 *Mater. Res. Express* **6** 116211

Materials Research Express

CrossMark

OPEN ACCESS

RECEIVED
17 July 2019

REVISED
20 September 2019

ACCEPTED FOR PUBLICATION
9 October 2019

PUBLISHED
18 October 2019

PAPER

Menger fractal structure with negative refraction and sound tunnelling properties

Yu Liu[1,2], Wenshuai Xu[1,2], Meng Chen[1,2,3], Dongliang Pei[1,2], Tao Yang[1,2], Heng Jiang[1,2,3] and Yuren Wang[1,2]

[1] Key Laboratory of Microgravity, Institute of Mechanics, Chinese Academy of Sciences, Beijing 100190, People's Republic of China
[2] University of Chinese Academy of Sciences, Beijing, 100049, People's Republic of China
[3] Authors to whom any correspondence should be addressed.

E-mail: chenmeng@imech.ac.cn and hengjiang@imech.ac.cn

Keywords: Menger fractal structure, negative refraction, acoustic focusing, sound tunnelling

Abstract

We construct new quasi-three-dimensional fractal acoustic metamaterials based on adoption of the Menger structure, which offers extraordinary parameters such as double-negative properties and a near-zero density. The resulting metamaterials can thus achieve negative refraction, acoustic focusing and sound tunneling. Using the finite element method and the S-parameter retrieval method, the band structures and the effective parameters of these acoustic metamaterials are researched, respectively. The negative refraction property is numerically simulated using a Gaussian beam passing through a double negative prism. A plate lens with a refractive index of $n = -1$ is constructed to achieve acoustic focusing and the sound tunnelling ability is verified using the near-zero-density metamaterial. The results show that the Menger fractal structures have excellent acoustic properties and are promising for acoustic applications.

1. Introduction

Negative refraction, acoustic focusing and sound tunneling have attracted the interest of many researchers because of the potential engineering applications of these unique physical properties [1–6]. These properties are achieved using artificial materials called metamaterials, which have extraordinary structural parameters that include negative effective mass density [7–11], negative effective bulk modulus [12] and double-negative properties [13–21]. These acoustic metamaterials are generally based on the principle of local resonance. To achieve the required double-negative properties, researchers usually combine the negative mass density structure with the negative bulk structure, but the resulting structures are complex and generally anisotropic with a low symmetry. Furthermore, it is still a considerably technological challenge to encapsulate the high-density particles in a soft matrix material with a highly stable shape and a well controllable arrangement, which seriously restrict their practical applications [22]. Because the negative mass density and the negative bulk modulus are caused by monopole resonance and dipole resonance, respectively, the double-negative properties can also be realized if a single structural unit has these two resonance modes; this structure will then be easier to apply.

Recently, several researchers have reported that labyrinthine fractal structures have demonstrated multiple resonance modes [22–32]. These structures are usually designed by coiling them up within a space; in this way, the transmission paths can be greatly increased and this produces an ultraslow transmission effect. Because of the increased lengths of the transmission paths, these metamaterials have high refractive indexes and have shown extraordinary acoustic properties. Liang *et al* constructed an extreme acoustic metamaterial by coiling it up in space using zigzag channels; the resulting materials had both negative refraction and sound tunneling properties [29]. Liu *et al* proposed an ultra-sparse metasurface for high-level reflection of low-frequency sound based on Mie resonance units [26]. Xia *et al* reported labyrinthine acoustic metamaterials with Hilbert fractal structures that could easily form low-frequency bandgaps and demonstrated multi-bandgap properties [24]. However, most acoustic metamaterials are designed in the form of 2D structures, which are not beneficial for

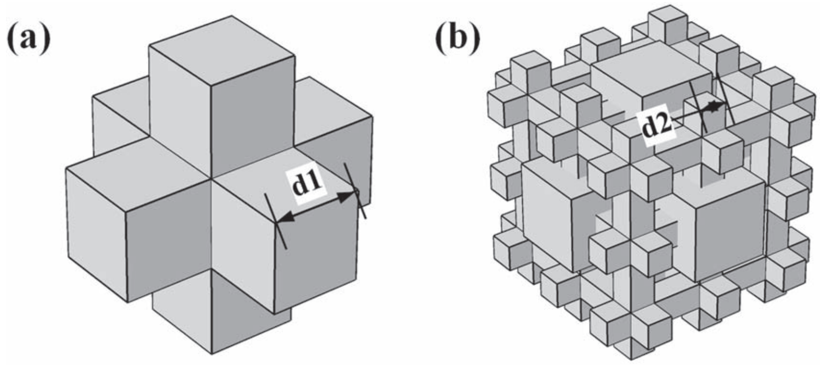

Figure 1. (a) Basic form of the Menger fractal structure. (b) Menger fractal structure studied in this text.

practical applications. Some researchers have also constructed 3D fractal metamaterials by coiling them up in space and have mainly studied the bandgap properties of these structures [33–36]. However, the structures fabricated in this manner are complex and this limits their applications in engineering. Compared with the locally resonant acoustic metamaterials and the space-coiling fractal metamaterials reported before, quasi-3D fractal metamaterials based on the Menger structure have high symmetry and multiple resonant modes, which can achieve double negative property with a single unit. Furthermore, quasi-3D Menger fractal structure can also act as the basis to combine with the Zigzag channels, which also provide a promising way to construct 3D space-coiling structure.

In this work, quasi-3D acoustic metamaterials with Menger fractal structures are constructed that have multiple resonance modes and negative refraction over a wide operating range. Using the finite element method and the S-parameter retrieval method, the band structures, the equivalent frequency surface (EFS) and the refractive indexes of these acoustic metamaterials are calculated. Acoustic lens are also constructed to achieve both negative refraction and acoustic focusing. Furthermore, the near-zero-density metamaterials are also used to verify the sound tunneling properties of the structures. The results show that these more easily constructed Menger structures have excellent acoustic properties and are promising for engineering applications.

2. Design of Menger fractal acoustic metamaterials

In order to show the construction process of Menger fractal structure clearly, we mainly show the sound tunnels of Menger structure in this text and the construction of the Menger structures' sound tunnels can be described in the following manner. The starting structure is a cube with side length **a** (72 mm) and each face of this cube is divided into nine squares; in this way, the cube is divided into 27 smaller cubes with side length **d1** (24 mm). Second, the middle cube of each face is selected and the most central cubes act as the acoustic tunnels, which consist of seven smaller cubes. In this way, we can construct the basic Menger fractal structure, as shown in figure 1(a). Then, using the method described above, we divide the remaining 20 smaller cubes with side length **d1** (24 mm) in the same manner and again select the middle cubes, which have a side length of **d2** (8 mm), to act as the acoustic tunnels. In this way we construct 20 smaller Menger fractal structures. Finally, the Menger fractal structure reported in this text consists of the 20 smaller Menger structures and the basic Menger structure and is illustrated in figure 1(b). The Menger fractal structure looks complicated, but it's easy to construct. Because there are only two different sizes of sound channels, the arrangement of the sound tunnels are also clear and the Menger fractal structures also have high symmetry. Compared with the 3D fractal acoustic metamaterials, the Menger fractal structure is simple and easy to be constructed. Furthermore, the figures show that the Menger fractal structures include multiple acoustic tunnels that can effectively reduce the reflection of acoustic waves at the acoustic metamaterial surface; they also demonstrate a better way to construct lightweight acoustic metamaterials, which are promising for applications in engineering.

3. Band structures and EFS of the Menger structure

To study the acoustic characteristics of the proposed Menger structure, we calculated and analyzed the band structures, which are illustrated in figure 2(a). The horizontal axis represents the values of the wave vector **k** along the borders (R-M-Γ–X–R) of the irreducible Brillouin zone of a cubic periodic lattice, while the vertical

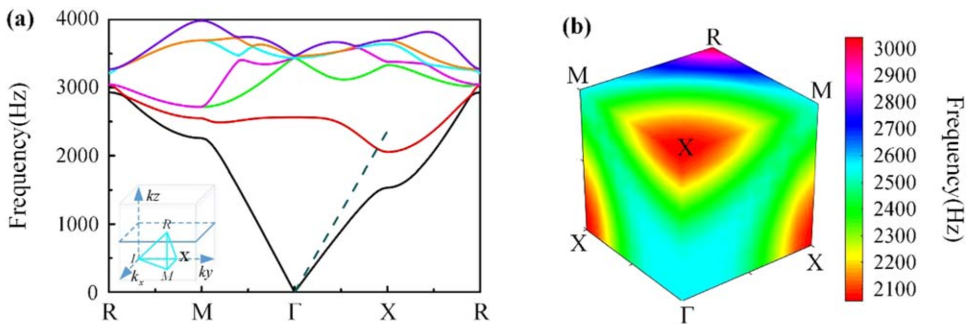

Figure 2. (a) Band structures of the Menger fractal acoustic metamaterial. (b) EFS of the Menger fractal acoustic metamaterial.

axis represents frequency. The results show that the slope of the second line in red in the ΓX direction is negative, which indicates that there are double-negative properties within the 2160 Hz–2560 Hz frequency range.

To enable further study and analysis of the double-negative characteristics of the Menger structure, we calculate the EFS of the Menger structure using the finite element method, with results as shown in figure 2(b), where the different frequencies are represented by different colours. According to equation (1), the gradient direction of the EFS is the direction in which the group velocities propagate within the Menger structure. The frequency declines in the ΓX direction, which indicates that the propagation of the group velocities (**S**) in the Menger structure is in the XΓ direction. Because the direction of the wave vector (**k**) is in the ΓX direction, this demonstrates that the wave vector and the group velocities have opposite directions and that $\mathbf{S}\cdot\mathbf{k} < 0$, thus verifying the double-negative properties of the proposed Menger structure.

$$v_g = \nabla_k w(k) = e_x \cdot \frac{\partial}{\partial k_x} w(k_x, k_y, k_z) + e_y \cdot \frac{\partial}{\partial k_y} w(k_x, k_y, k_z) + e_z \cdot \frac{\partial}{\partial k_z} w(k_x, k_y, k_z) \quad (1)$$

4. Calculation of effective parameters

To provide a better understanding of the diagram of the double-negative property formation, we calculated the effective parameters of the fractal acoustic metamaterial using the S-parameter retrieval method [37]. The effective mass density, the bulk modulus and the refractive index of the material are calculated as follows:

$$\rho_{eff} = \varepsilon \times n \quad (2)$$

$$B_{eff} = \frac{\varepsilon}{n} \quad (3)$$

When using the S-parameter retrieval method, ε and n can be expressed as follows:

$$\varepsilon = \frac{r}{1 - 2R + R^2 - T^2} \quad (4)$$

$$\mathrm{n} = \frac{-i \log x + 2\pi m}{kd} \quad (5)$$

where

$$\mathrm{r} = \mp\sqrt{(R^2 - T^2 - 1)^2 - 4T^2} \quad (6)$$

$$\mathrm{X} = \frac{(1 - R^2 + T^2 + r)}{2T} \quad (7)$$

In the above formulation, R is the reflection coefficient of the structure and T is the transmission coefficient of the structure; these properties are calculated using COMSOL Multiphysics software. In this way, the refractive index, effective mass density and bulk modulus of the fractal metamaterial can be calculated, as shown in figures 3(c) and (d). The results show that within the frequency range of the negative slope (2160 Hz–2560 Hz), the effective mass density, the bulk modulus and the refractive index are all negative simultaneously and are well matched with each other; this proves that the quasi-3D fractal acoustic metamaterial has excellent double-negative properties.

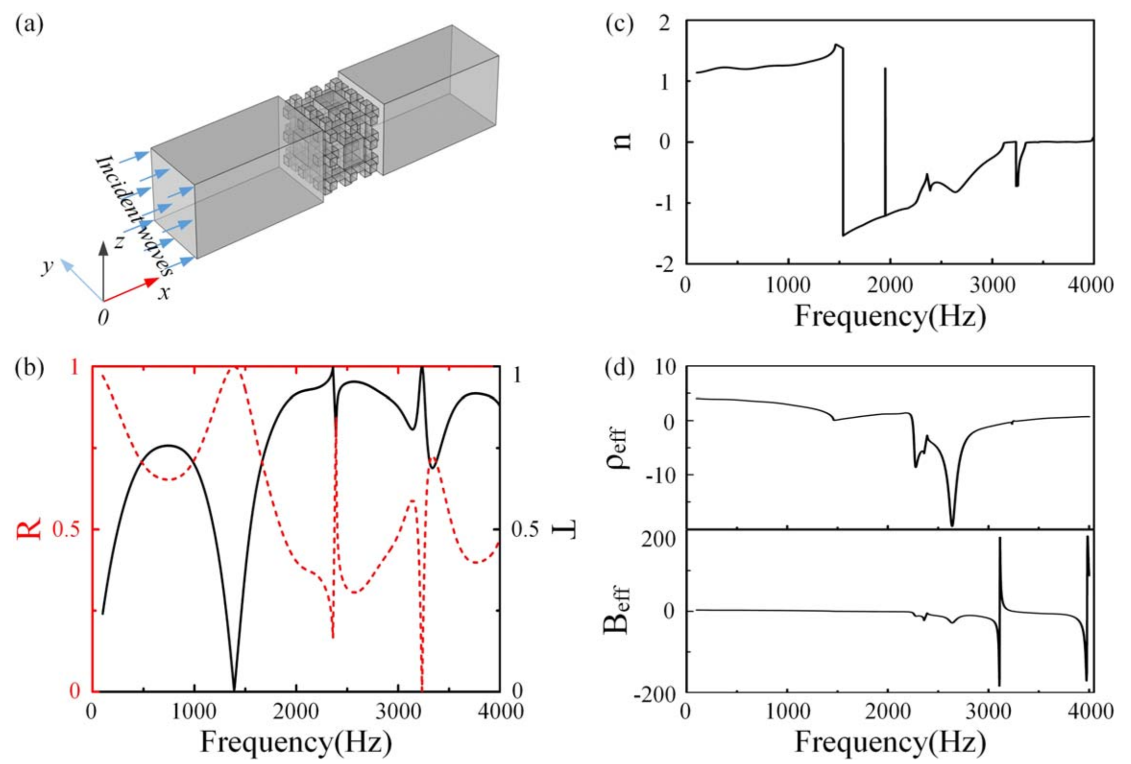

Figure 3. (a) Simulation model (b) Reflection and transmission coefficients of the fractal acoustic structures (c) Refractive index. (d) Effective mass density and bulk modulus characteristics.

5. Extraordinary acoustic properties

The results of the calculations of the band structures and the effective parameters show that within the 2160–2560 Hz frequency range, the effective parameters of the Menger structure are negative. The structure also has a near-zero density at a frequency of 3274 Hz. These extraordinary parameters indicate that the Menger fractal structure has excellent acoustic properties such as negative refraction, acoustic focusing and sound tunneling. To provide further verification of these properties, we adopt the Finite element methods (FEMs), which are commonly used to calculate the band structure and vibration modes of acoustic metamaterials and the FEM software COMSOL Multiphysics was used to calculate the band structure, effective parameters and transmission response of the quasi-3D Menger fractal acoustic metamaterials in this paper. Because of the high symmetry of the Menger fractal structure, the calculation can be simplified in the x-z planes. Therefore, we build the calculation model in the x-z planes, acoustic waves propagate along the x-axis and mainly study the phenomena in the x-z planes.

To verify the negative refraction property, we constructed an acoustic prism that had negative density and negative bulk modulus simultaneously. For the negative refraction, we selected 45 units to construct the prism with a 45-unit wedged structure and the PML were added in the boundary to eliminate the influence of acoustic waves' reflection. A Gaussian acoustic pulse with unit amplitude then impinged on the prism from the left along the ΓX direction toward the right at a frequency of 2205 Hz, at which the relative effective refractive index is -1. The results are shown in figure 4. After passing through the lens, the sound wave no longer continues to propagate horizontally; instead, the propagation direction changes to upward. The direction of incidence and the refraction direction of the sound wave are on the same side of the normal line, which indicates that the acoustic lens formed using the Menger metamaterials can achieve negative refraction. These results match the results for the band structures and the refractive indexes well and thus verify the double-negative characteristics of the Menger metamaterial structure.

The above research shows that the Menger structure has the negative refraction property and acoustic focusing is one of the most important applications of negative refraction. To achieve acoustic focusing, we constructed a plate lens with refractive index of $n = -1$ at a frequency of 2205 Hz, where the thickness and the width of the plate lens were 4 units and 20 units, respectively and the PML were added in the boundary to eliminate the influence of acoustic waves' reflection. A point wave source was then placed at a distance of 2a from the left surface of the slab. The incident wave was emitted by a point source at a frequency of 2205 Hz and the numerical simulation results are shown in figure 5(a). We can see a clear image point whose acoustic pressure is

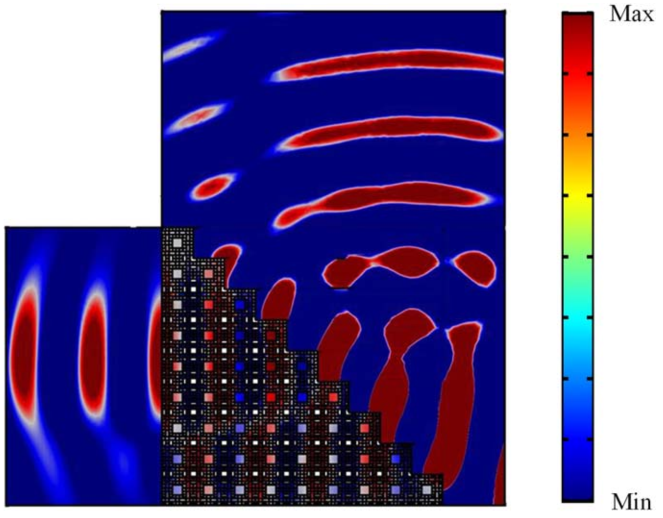

Figure 4. Sound pressure pattern with an acoustic prism with Menger fractal structure.

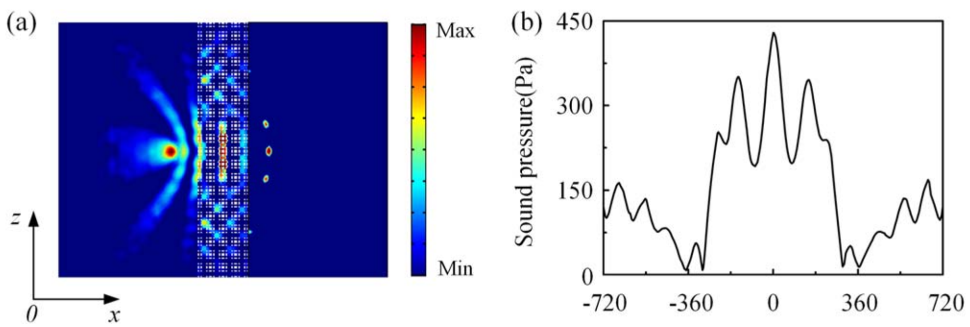

Figure 5 (a) Distribution of the simulated sound pressure around the plat lens. (**b**) Sound pressure distribution at the image point along the Z direction.

much larger than the others on the right of the lens, which is approximately 2a away from the right surface of the lens. The distance from the source to the image is approximately twice the lens thickness, which matches well with the results from acoustic ray tracing theory [22]. We also calculated the acoustic pressure distribution along the z direction at a distance of 2a from the right surface of the slab for further study, with results as shown in figure 5(b). The central acoustic pressure is much larger than that on either side, which also serves as strong proof that the plate lens can achieve acoustic focusing. There are also two relatively larger side lobes, whose locations match well with the two smaller points which distribute in both sides of the focusing point. These results serve as strong proof that the plate lens can achieve acoustic focusing.

The Menger structure not only has negative effective parameters, but also has a near-zero-density at the frequency of 3274 Hz, which can be used to realize acoustic tunneling effects. To verify this acoustic property of the Menger structure, we established an acoustic transmission model and performed a numerical simulation analysis using COMSOL Multiphysics software. In figure 6(a), plane acoustic waves propagate from the left toward the right along the sound tunnel, and while the tunnel becomes narrow at its centre, the sound waves can continue to travel as plane waves. For comparison, we calculated the same results using the traditional structure; the results are shown in figure 6(b) and indicate that the sound waves are strongly scattered in places in the narrow channel and also provide further proof that the Menger structure has the sound tunnelling property.

6. Conclusions

In this work, quasi-3D Menger fractal acoustic metamaterials are proposed and the extraordinary acoustic properties of these materials, including negative refraction, acoustic focusing, and sound tunnelling are studied systematically by calculating their band structures, their EFSs and their effective parameters and then performing numerical simulations. The results show that first, in the frequency range of the negative slope

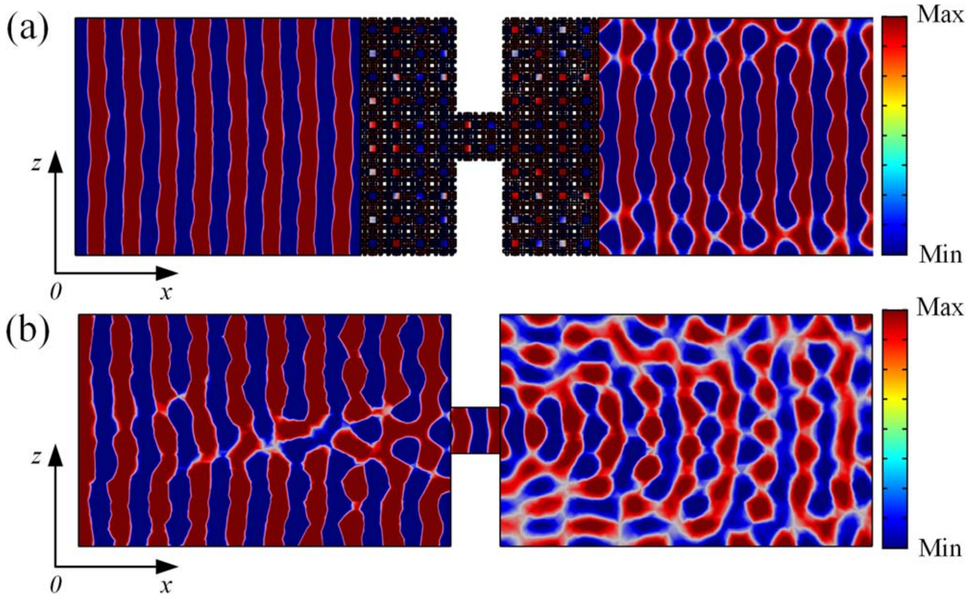

Figure 6. (a) Sound pressure distribution when the acoustic waves propagate through a narrow channel filled with Menger fractal structure. (b) Sound pressure distribution when the acoustic waves propagate through a narrow channel filled without Menger fractal structure.

shown in the second band, the group velocities and the wave vector are in opposite directions, which proves that the Menger fractal structure can achieve negative refraction. Second, in the negative refraction frequency range, the effective mass density and the bulk modulus are both negative, which is the key factor that allows the Menger fractal structure to achieve its negative properties. Furthermore, the numerical simulations also showed that the Menger structure has multiple excellent acoustic properties. Unlike the traditional space-coiling fractal metamaterials and locally resonant metamaterials, the Menger structure not only has extraordinary acoustic properties but also has larger numbers of sound tunnels, which can reduce both acoustic reflection and the overall weight of the structure, and these materials are thus promising for applications in engineering.

Acknowledgments

The authors acknowledge that this project was supported by the National Natural Science Foundation of China (Grant Nos. 11602269 and 11802213), the Strategic Priority Research Program of the Chinese Academy of Sciences (Grant No. XDB22040301) and the Research Program of Beijing (Grant Nos. Z161100002616034 and Z171100000817010).

ORCID iDs

Heng Jiang https://orcid.org/0000-0002-6552-2809

References

[1] Nemat-Nasser S 2019 *Mech. Mater.* **132** 1–8
[2] Zhang X and Liu Z 2004 *Appl. Phys. Lett.* **85** 341–3
[3] Feng L, Liu X P, Chen Y B, Huang Z P, Mao Y W, Chen Y F and Zhu Y Y 2005 *Phys. Rev.* B **72** 033108
[4] Mokhtari A A, Lu Y and Srivastava A 2019 *J. Mech. Phys. Solids.* **126** 256–71
[5] Zhu R, Liu X N, Hu G K, Sun C T and Huang G L 2014 *Nat. Commun.* **5** 5510
[6] Notomi Á 2000 *Phys. Rev.* B **62** 10696
[7] Liu Z, Zhang X, Mao Y, Zhu Y Y, Yang Z, Chan C T and Sheng P 2000 *Science* **289** 1734–6
[8] Hirsekorn M 2004 *Appl. Phys. Lett.* **84** 3364–6
[9] Wang G, Wen X, Wen J, Shao L and Liu Y 2004 *Phys. Rev. Lett.* **93** 154302
[10] Hsu J C and Wu T T 2007 *Appl. Phys. Lett.* **90** 201904
[11] Sainidou R, Djafari-Rouhani B, Pennec Y and Vasseur J O 2006 *Phys. Rev.* B **73** 024302
[12] Fang N, Xi D, Xu J, Ambati M, Srituravanich W, Sun C and Zhang X 2006 *Nat Mater* **5** 452
[13] Li J and Chan C T 2004 *Phys. Rev.* E **70** 055602
[14] Ding Y, Liu Z, Qiu C and Shi J 2007 *Phys. Rev. Lett.* **99** 093904
[15] Lee S H, Park C M, Seo Y M, Wang Z G and Kim C K 2010 *Phys. Rev. Lett.* **104** 054301

[16] Chen H, Zeng H, Ding C, Luo C and Zhao X 2013 *J. Appl. Phys.* **113** 104902
[17] Zeng H C, Luo C R, Chen H J, Zhai S L, Ding C L and Zhao X P 2013 *Solid. State. Commun.* **173** 14–8
[18] Chen H, Li H, Zhai S, Ding C, Li J, Luo C and Zhao X 2016 *J. Appl. Phys.* **119** 204902
[19] Fok L and Zhang X 2011 *Phys. Rev.* B **83** 214304
[20] Lai Y, Wu Y, Sheng P and Zhang Z Q 2011 *Nat. Mater.* **10** 620
[21] Yang M, Ma G, Yang Z and Sheng P 2013 *Phys. Rev. Lett.* **110** 134301
[22] Xia B, Li L, Liu J and Yu D 2018 *J. Vib. Acoust.* **140** 011011
[23] Liu J, Li L, Xia B and Man X 2018 *Int. J. Solids Struct.* **132** 20–30
[24] Man X, Liu T, Xia B, Luo Z, Xie L and Liu J 2018 *J. Sound Vib.* **423** 322–39
[25] Krushynska A O, Bosia F, Miniaci M and Pugno N M 2017 *New J. Phys.* **19** 105001
[26] Cheng Y, Zhou C, Yuan B G, Wu D J, Wei Q and Liu X J 2015 *Nat Mater* **14** 1013
[27] Krushynska A O, Bosia F and Pugno N M 2018 *Acta Acust. United Ac.* **104** 200–10
[28] Miniaci M, Krushynska A, Gliozzi A S, Kherraz N, Bosia F and Pugno N M 2018 *Phys. Rev. Appl.* **10** 024012
[29] Liang Z and Li J 2012 *Phys. Rev. Lett.* **108** 114301
[30] Liang Z, Feng T, Lok S, Liu F, Ng K B, Chan C H and Li J 2013 *Sci. Rep.* **3** 1614
[31] Li Y, Liang B, Tao X, Zhu X F, Zou X Y and Cheng J C 2012 *Appl. Phys. Lett.* **101** 233508
[32] Zigoneanu L, Popa B I and Cummer S A 2011 *Phys. Rev.* B **84** 024305
[33] Fu X F, Li G Y, Lu M H, Lu G and Huang X 2017 *Appl. Phys. Lett.* **111** 251904
[34] Frenzel T, David Brehm J, Bückmann T, Schittny R, Kadic M and Wegener M 2013 *Appl. Phys. Lett.* **103** 061907
[35] Zhang C and Hu X 2016 *Phys. Rev. Appl.* **6** 064025
[36] Man X, Xia B, Luo Z and Liu J 2019 *J. Phys. D Appl. Phys.* (https://doi.org/10.1088/1361-6463/ab092a)
[37] Fokin V, Ambati M, Sun C and Zhang X 2007 *Phys. Rev.* B **76** 144302